



Solvation Dynamics of Oxadiazoles as Potential Candidate for Drug Preparation

VIKASH KUMAR^{id}, RAVINDRA KUMAR^{id}, NAGENDRA KUMAR^{id} and SUMIT KUMAR^{*id}

Department of Chemistry, Magadh University, Bodh Gaya-824234, India

*Corresponding author: E-mail: sumitkrmgr@gmail.com

Received: 22 January 2023;

Accepted: 6 March 2023;

Published online: 30 March 2023;

AJC-21200

Oral ingestion is one of the popularly employed procedures for the drug delivery as the administration of drugs is easy compared to the other alternatives such as injection. Therefore, the drug preparation is affected by dissolution rate, metabolism as per system requirements, drug permeability as well as solubility of the drug. The current study focused on the solvation dynamics of oxadiazole derivatives to attain its candidature against drug preparation. Different derivatives are extensively explored using *ab initio* molecular dynamics and quantum chemical calculation tools. The molecular dynamics study depicts the total energy as the addition of kinetic as well as potential energies with the progress of simulation time in fs. Oxadiazole derivative solvation efficiency was also investigated, along with its main solvent interaction sites. Derivatives of 1,3,4-oxadiazole were analyzed to determine their band gap energies, softness, hardness, ionization potential, chemical potential, electrophilicity, nucleophilicity, electronegativity and also their pharmacological effects.

Keywords: Solvation dynamics, Oxadiazoles, Drug, ADME, Fukui, Hard and soft acid base theory.

INTRODUCTION

Oxadiazoles are the five-membered ring structures adjusting one oxygen along with two nitrogen atoms. Some major applications are reported in the crucial drugs such as raltegravir, zibotentan, fenadiazole and tiadazosin [1-7]. Raltegravir is used in an antiretroviral medication for human immuno-deficiency viruses (HIV) whereas zibotentan is a potential candidate for the manufacturing of drugs having anticancer properties developed by Astra Zeneca [8,9]. Fenadiazole is used as hypnotic drug whereas tiadazosin used as a receptor antagonist [10]. Moreover, oxadiazole derivatives have widespread applications in numerous fields such as electron transporting materials, corrosion inhibitors, polymers and luminescence producing materials [11-14].

Oral ingestion is one of the popularly employed procedures for the drug delivery as the administration of drugs is easily comparable to the other alternatives such as injection [15,16]. Furthermore, the high compliance rate to the patient for the oral ingestion is due to cost effectiveness as well as flexibility to manipulate the drug doses. Interestingly, this attracted a lot of drug companies to produce generic medicines and therefore the market of these medicines is in billions. But the challenges

are majorly faced by poor bioavailability. It is affected by dissolution rate, metabolism as per system requirements, drug permeability as well as solubility of the drug. A poor solubility of the drug almost affects all properties depending upon the environment. Therefore, the solubility of the drug is of major interest in the current scenario.

Keeping this in mind, to determine the pharmacokinetic profile of each compound, a comprehensive virtual screening study was devised, including density functional theory (DFT) analysis to determine the compounds solubility and reactivity, molecular docking to estimate binding affinity in order to confirm the solubility, *ab initio* molecular dynamic simulations and ADMET properties of 1,3,4-oxadiazoles. Eventually the *ab initio* molecular dynamics (AIMD) of oxadiazole has been studied to obtain in-depth understanding effect of solvent (water) environment. The study may be helpful to tailor the structure functional related properties of oxadiazoles based drugs.

EXPERIMENTAL

A representative collection of nine structures of oxadiazole derivatives was performed through density functional theory (DFT). The chemical calculations utilize the def2-SVP basis

set along with B3LYP functional. The basis set can accurately determine the energy associated with highest occupied molecular orbital (HOMO) lowest unoccupied molecular orbital (LUMO), electronegativity, electrophilicity, hardness, softness, proton affinity and nucleophilicity. These calculations are performed using ORCA 5.0.3 program suite [17,18]. The Fukui function has been calculated by using the local molecular reactivity using eqn. 1 [19,20]:

$$f(\vec{r}) = \left(\frac{\rho(\vec{r})}{\partial N} \right) V(\vec{r}) \quad (1)$$

where ρ , N and $V(\vec{r})$ define the electronic density, number of electron and external potential associated with molecular system, respectively. The study has been performed by the removal and addition of electrons from the molecular systems using eqns. 2 and 3 [21]:

$$\rho^-(\vec{r}) \approx \rho_{\text{LUMO}}(\vec{r}) \quad (2)$$

$$\rho^+(\vec{r}) \approx \rho_{\text{HOMO}}(\vec{r}) \quad (3)$$

where $\rho_{\text{LUMO}}(\vec{r})$ and $\rho_{\text{HOMO}}(\vec{r})$ are the the electron density for LUMO and HOMO, respectively. Further, the molecular local activity site incorporates infinitesimal change in the quantum computational calculation achieved from Mulliken population analysis changes. Fukui function has been used to isolate the information related to two types of local active sites, electrophilic and nucleophilic. To understand, the behaviour of various substituted oxadiazoles, various substitutions of functional groups take place at the second and fourth positions (Fig. 1).

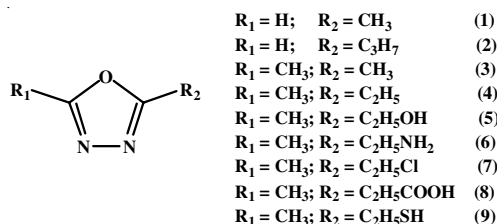


Fig. 1. Chemical structure of 1,3,4-oxadiazole derivatives with substitutions R_1 and R_2

The electron withdrawing as well as donating functional groups such as methyl (-CH₃), ethyl (-C₂H₅), propyl (-C₃H₇), hydroxyethyl (-C₂H₅OH), chloroethyl (-C₂H₅-Cl), carboxyethyl (-C₂H₅-COOH) and thioethyl (-C₂H₅-SH) and aminoethyl (-C₂H₅-NH₂) were considered for R_1 and R_2 substitution. These compounds are abbreviated as oxa1, oxa2, oxa3, oxa4, oxa5, oxa6, oxa7, oxa8 and oxa9, respectively.

Computational studies: DFT quantum calculations were performed to optimized various geometry of substituted 1,3,4-oxadiazoles by TURBOMOLE 7.6 program suite [22,23]. Some related parameters such as band gap energies, softness, hardness, ionization potential, chemical potential, electrophilicity, nucleophilicity and electronegativity of different derivatives of 1,3,4-oxadiazole were computed using ORCA 5.0.3 [17,18]. The MD calculations were also performed using ORCA 5.0.3 software and the solvated properties of the oxadiazoles were studied. The pharmacological properties have been predicted with BOILED-Egg representation obtained from SWISS-ADME software [24-26].

RESULTS AND DISCUSSION

Quantum chemical calculations

HOMO–LUMO energy gaps: A summary of HOMO and LUMO of optimized structures of substituted oxadiazole derivatives **1-9** is shown in Table-1. As the energy of HOMO goes higher the tendency to donate electrons increases, this is due to the decrease of the energy gap with the LUMO. Further, the decrease in the orbital energy of LUMO increases the tendency to accept electrons. Thus, the flow of electrons affected by the band gap determines the solvation property of oxadiazole derivatives.

Fukui function calculations and molecular properties: Various quantum calculation parameters such as chemical potential, electronegativity, electrophilicity, nucleophilicity and chemical hardness were used to study computational properties. Koopmans theorem was employed to explain the hard and soft acid-base theory. The theory is extended by the Pearson model to describe the HSAB theory, which discusses soft-soft and hard-hard interactions. This parameter appends upon chemical potential, hardness and another related parameters as described below:

$$I = -E_{\text{HOMO}} \quad (4)$$

$$A = -E_{\text{LUMO}} \quad (5)$$

$$\chi = \left(I + \frac{A}{2} \right) \quad (6)$$

$$\eta = I - \frac{A}{2} \quad (7)$$

$$\sigma = \frac{1}{\eta'} \quad (8)$$

$$\omega = \frac{\mu^2}{\eta'} \quad (9)$$

For a high reactivity of the chemical species, the band gap energy should be low as a hard molecule shows lower reactivity in comparison to a soft molecule because a soft molecule has a low band gap. Thus, the reactivity combined with the stability of the molecular system depends upon hardness and softness. The property of the molecular system hardness is also associated with the deformation of the molecular system by applying a low perturbation.

The small band gap energy for a chemical species makes it more reactive and a soft molecule has small band gap energy whereas a large band gap can be seen for hard molecular system therefore the reactivity and stability of chemical species can be predicted from the hardness and softness of the molecular systems [27]. The softness of the compound relays on easy deformation of the electron cloud where as a hardness of the molecular system prevent the deformation and polarization of the electron cloud of the molecular system [28]. Thus, interaction efficiency with solvent can be calculated with the softness of the molecule and higher the efficiency can be supported from higher softness of the molecular system [29].

TABLE-1
OPTIMIZED STRUCTURES ALONG WITH HOMO AND LUMO OF 1,3,4-OXADIAZOLE
NON-PROTONATED INHIBITOR MOLECULES 1 TO 9 IN GAS PHASE

	Structure	HOMO	LUMO
oxa1			
oxa2			
oxa3			
oxa4			
oxa5			
oxa6			
oxa7			
oxa8			
oxa9			

The quantum computational calculation of 1,3,4-oxadiazole derivatives were performed in the gas phase. The chemical potential, chemical hardness, chemical softness, electronegativity and electrophilicity for oxadiazole derivatives are shown in Table-2. In gaseous phase, the LUMO energy varies with the order: oxa1 < oxa2 < oxa3 < oxa4 < oxa7 < oxa5 < oxa8 < oxa9 < oxa6, whereas the orbital energy associated with the HOMO charges according to the trend; oxa1 < oxa3 < oxa4 < oxa2 < oxa5 < oxa7 < oxa8 < oxa6 < oxa9. The orbital energy associated with HOMO and LUMO describes the ionization energy and electron affinity of the molecule. Thus, the trends for ionization energy is oxa9 < oxa6 < oxa8 < oxa7 < oxa5 < oxa2 < oxa4 < oxa3 < oxa1 whereas the trend for electron affinity is oxa6 < oxa8 < oxa5 < oxa7 < oxa4 < oxa3 < oxa2 < oxa1. The HOMO energy depends upon the ionization energy depicts the tendency of donating electrons and the LUMO energy decreases with the tendency of accepting electrons and therefore electron affinity of the molecular system. The orbital energy band gap is calculated and formed according to the trend oxa2 < oxa7 < oxa9 < oxa4 < oxa3 < oxa8 < oxa6 < oxa5 < oxa1, smaller the band gap the reactivity of the molecule increases. Thus, following the trend, oxa1 shows the highest band gap whereas oxa2 is the lowest. This means that the oxa1 is the least and oxa2 is the highest reactive molecular species in the gaseous phase.

From the data of oxadiazole derivatives in aqueous phase (Table-3), it was found that LUMO varies with the order: oxa1 < oxa2 < oxa4 < oxa3 < oxa7 < oxa8 < oxa5 < oxa9 < oxa6, whereas the trend for the HOMO in aqueous phase was oxa1

< oxa3 < oxa4 < oxa2 < oxa5 < oxa8 < oxa7 < oxa9 < oxa6. Interestingly, the orbital energy band gap in aqueous phase incorporating the essence of both HOMO and LUMO energies follows the trend: oxa7 < oxa8 < oxa9 < oxa2 < oxa6 < oxa5 < oxa4 < oxa1 < oxa3. Therefore, the most reactive molecular species in the aqueous phase is oxa7, whereas the least reactive chemical species is oxa3.

The reactivity and stability of a molecular system can also be predicted from the softness and hardness of the molecular system [30,31]. The trend of observed for the softness of the oxadiazole derivative is oxa1 < oxa5 < oxa6 < oxa8 < oxa3 < oxa4 < oxa9 < oxa7 < oxa2. Furthermore, the trend of softness in the aqueous phase is oxa3 < oxa1 < oxa4 < oxa5 < oxa6 < oxa2 < oxa9 < oxa8 < oxa7. This provides the sufficient data to adopt a particular chemical species to understand the inter-action of solvent with oxadiazole derivatives in the aqueous environment.

The electrophilic and nucleophilic Fukui functions determines the interaction with water solvent (Figs. 2 and 3). Further indepth analysis of the solvent interaction is depicted in Fig. 4. The Mulliken charges decreases significantly on both nitrogen atoms present in the ring for oxadiazole derivatives on addition of water whereas no change is observed on oxygen atom. Similarly, the value of Fukui functions decreases significantly on both nitrogen atoms present in the ring for oxadiazole derivatives on addition of water whereas no change is observed on the oxygen atom. This modulates the interaction of nucleophile and electrophile to the ring of oxadiazole derivatives.

Electrostatic potential map: Fig. 5 shows the electrostatic potential (ESP) map for oxadiazole derivatives. The ESP

TABLE-2
MOLECULAR CHARACTERISTIC OF COMPOUNDS 1-9 OF 1,3,4-OXADIAZOLE DERIVATIVES IN GAS PHASE

Compound	oxa1	oxa2	oxa3	oxa4	oxa5	oxa6	oxa7	oxa8	oxa9
LUMO (eV)	-7.49	-7.15	-7.01	-6.79	-6.00	-5.17	-6.28	-5.80	-5.41
HOMO (eV)	-14.96	-13.74	-14.08	-13.85	-13.17	-12.31	-12.98	-12.91	-12.12
I (eV)	14.96	13.74	14.08	13.85	13.17	12.31	12.98	12.91	12.12
A (eV)	7.49	7.15	7.01	6.79	6.00	5.17	6.28	5.80	5.41
ΔE (eV)	7.46	6.59	7.06	7.06	7.17	7.13	6.70	7.12	6.71
η	3.73	3.29	3.53	3.53	3.58	3.57	3.35	3.56	3.35
σ	0.27	0.30	0.28	0.28	0.28	0.28	0.30	0.28	0.30
χ	11.23	10.44	10.54	10.32	9.58	8.74	9.63	9.35	8.77
CP	-11.23	-10.44	-10.54	-10.32	-9.58	-8.74	-9.63	-9.35	-8.77
ω	33.77	33.12	31.47	30.19	25.62	21.42	27.69	24.59	22.92
ϵ	0.27	0.30	0.28	0.28	0.28	0.28	0.30	0.28	0.30

TABLE-3
MOLECULAR CHARACTERISTIC OF COMPOUNDS 1-9 OF 1,3,4-OXADIAZOLE DERIVATIVES IN AQUEOUS SOLUTION

Compound	oxa1	oxa2	oxa3	oxa4	oxa5	oxa6	oxa7	oxa8	oxa9
LUMO (eV)	-2.803	-2.682	-2.423	-2.465	-1.886	-0.693	-2.406	-2.169	-1.128
HOMO (eV)	-10.146	-9.574	-9.801	-9.751	-9.083	-7.824	-8.606	-8.752	-7.867
I	10.146	9.574	9.801	9.751	9.083	7.824	8.606	8.752	7.867
A	2.803	2.682	2.423	2.465	1.886	0.693	2.406	2.169	1.128
ΔE (eV)	7.343	6.892	7.378	7.286	7.197	7.131	6.200	6.583	6.739
η	3.672	3.446	3.689	3.643	3.599	3.566	3.100	3.292	3.370
σ	0.272	0.290	0.271	0.274	0.278	0.280	0.323	0.304	0.297
χ	6.475	6.128	6.112	6.108	5.485	4.259	5.506	5.461	4.498
CP	-6.475	-6.128	-6.112	-6.108	-5.485	-4.259	-5.506	-5.461	-4.498
ω	11.417	10.897	10.126	10.241	8.359	5.086	9.779	9.059	6.003
ϵ	0.272	0.290	0.271	0.274	0.278	0.280	0.323	0.304	0.297

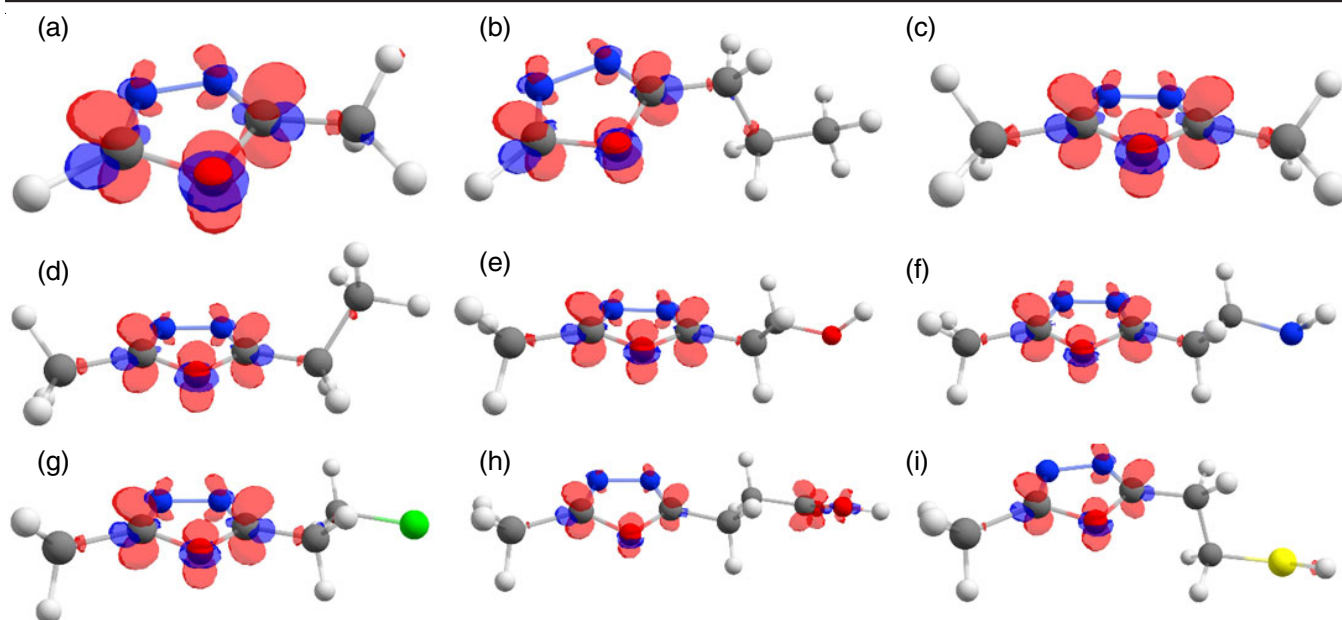


Fig. 2. Fukui functions (f_k^-) for compounds **1-9** of 1,3,4-oxadiazole plotted in (a)-(i), respectively

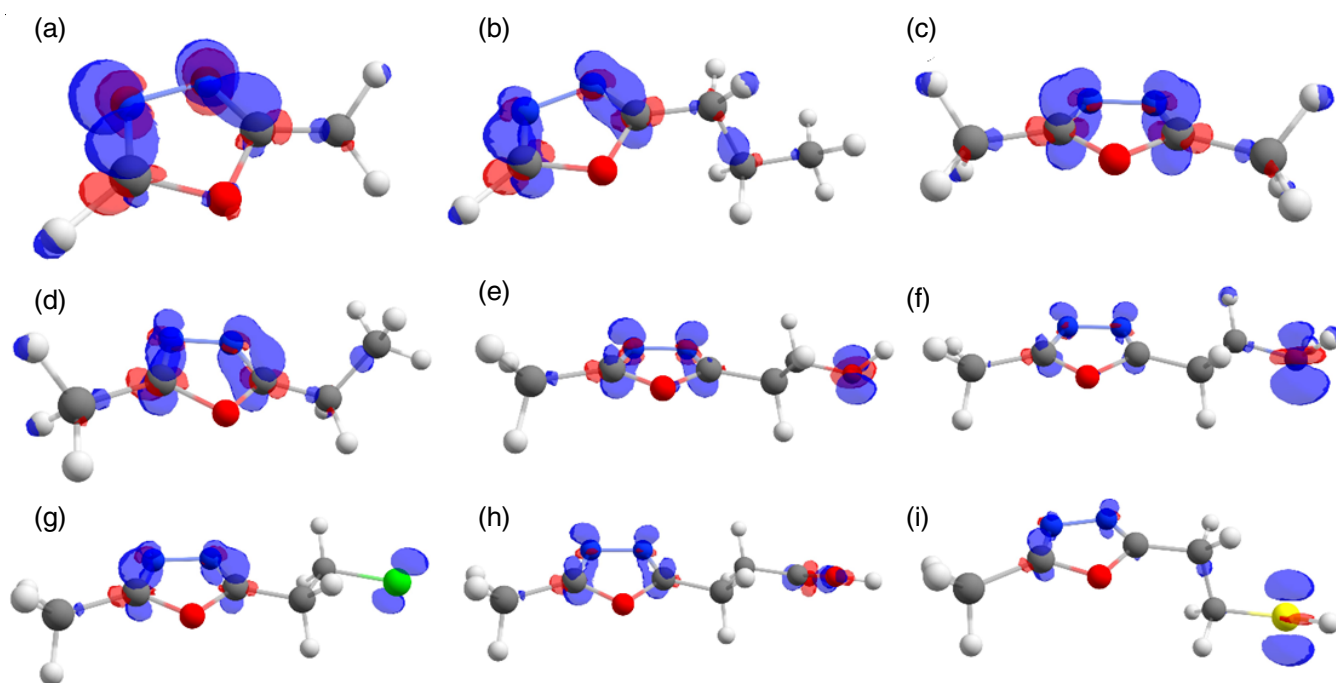


Fig. 3. Fukui functions (f_k^+) for compounds **1-9** of 1,3,4-oxadiazole plotted in (a)-(i), respectively

plot shows electrostatic potential based on the quantum calculations, which provides the reliable information regarding the chemical reaction related to the solvent interaction. The colour scheme in ESP plot shows red colour for the maximum whereas blue colour for minimum potential. The electron withdrawing and the electron donating groups play the significant role in deciding the presence of electron cloud across the molecule. The ESP plot correlates well with the data reported in Fig. 6.

ab initio Molecular dynamics (MD) studies: Molecular dynamics (MD) study was performed for oxadiazole derivatives with water using ORCA 5.0.3 software. The calculation was performed using Timestep of 1.0 fs at 350 K and Timecon of

10.0 fs. The simulation of oxadiazole derivatives with solvent (water) measured the total energy as the addition of kinetic as well as potential energies with change of simulation time in fs. Two major sites have been located for the solvent interaction for oxadiazole derivative *viz.* oxa1-wtr1 and oxa1-wtr2. The site of the interaction could be from either oxygen or nitrogen present in the oxadiazole ring. Oxa1-wtr1 corresponds to solvent interaction along nitrogen whereas solvent interaction along oxygen is related to oxa1-wtr2. The lowest decomposition energies for oxa1, oxa1-wtr1 and oxa1-wtr2 measured were -301.007505, -377.351497 and -377.345877 a.u., respectively. Interestingly, the electrostatic potential map set are in

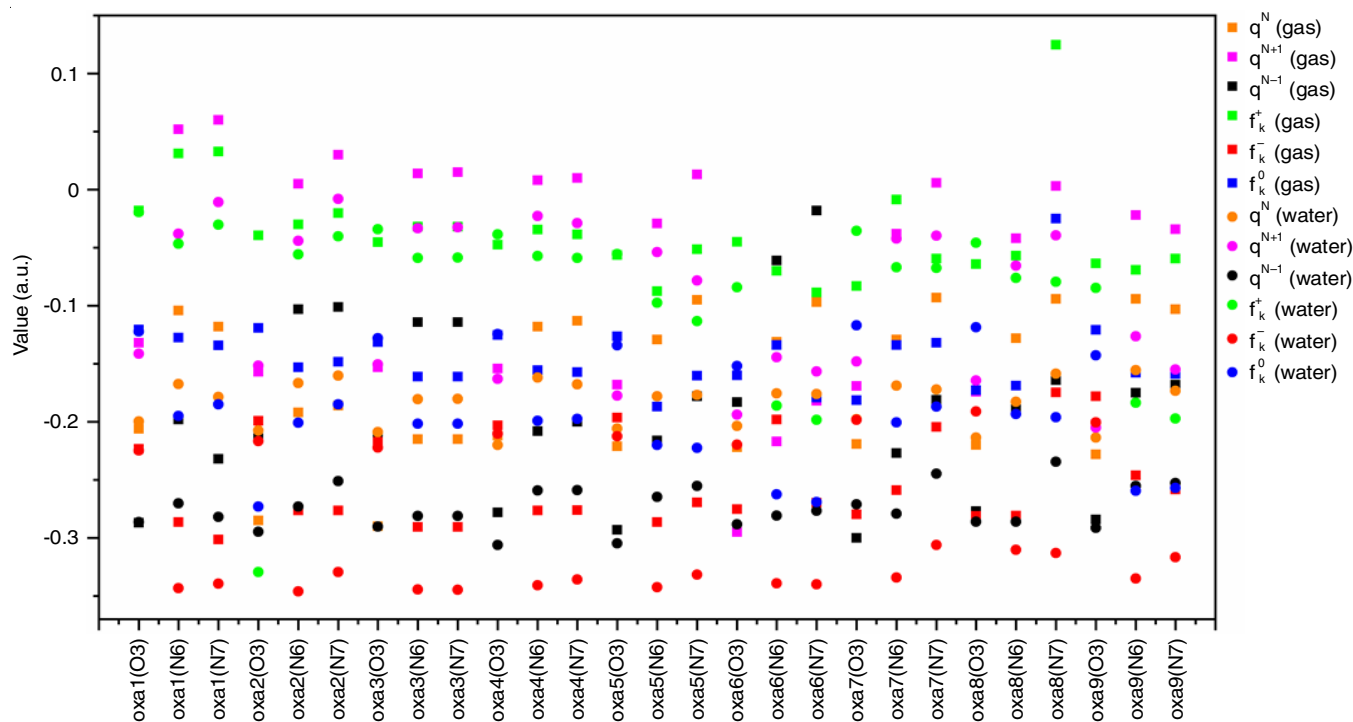


Fig. 4. Gas phase and aqueous phase calculations of Fukui functions and Mulliken atomic charges of 1,3,4-oxadiazole derivatives 1-9

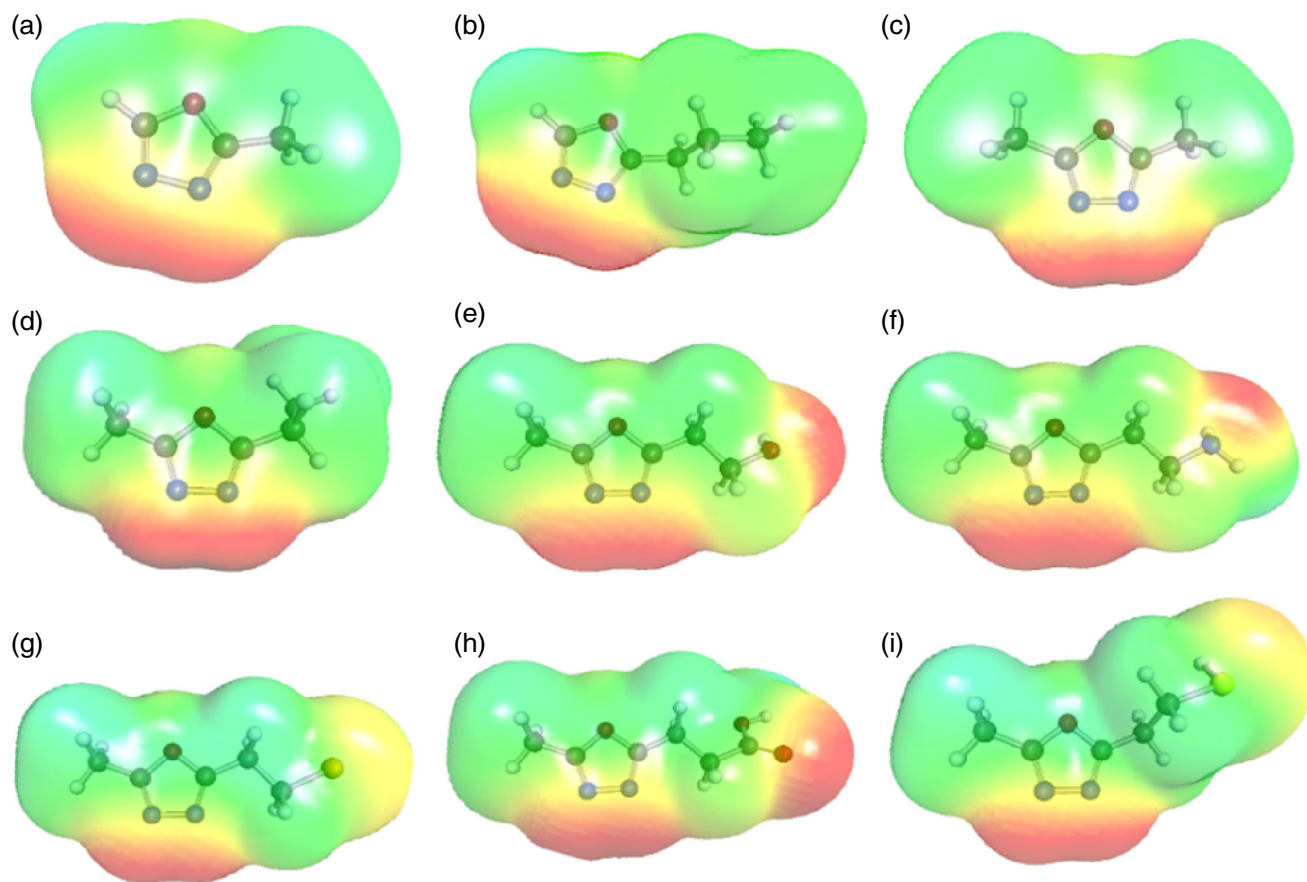


Fig. 5. Electrostatic potential (ESP) map for oxa1-9 shown in (a)-(i)

resemblance with the MD results. The MESP sigma hole calculation for oxadiazole was calculated and found to be -0.065 as well as $0.045e$ at nitrogen and oxygen, respectively.

Furthermore, the stability of solvent (water) is found along the nitrogen moiety of the oxadiazole ring, which corresponds well with MESP calculations.

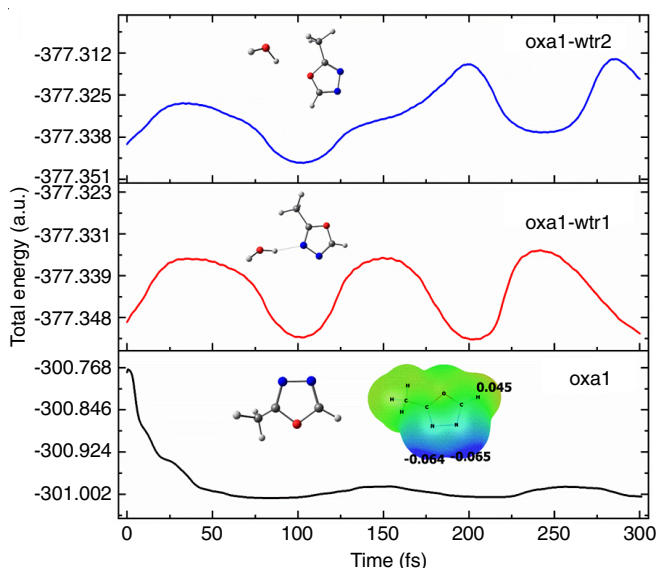


Fig. 6. Total energy during molecular dynamics study including MESP sigma hole calculation, for oxadiazole derivative (oxa1) with water

Pharmacokinetics and pharmacology properties: Fig. 7 represents a BOILED-Egg representation to investigate the gastrointestinal absorption as well as brain penetration of oxadiazole derivatives. Yellow egg's yolk represents the blood-brain barrier (BBB) permeation, which predicts the passively permeation through the blood-brain barrier. BOILED-egg's white in the figure corresponds to human intestinal absorption (HIA) data, which predicted to be passively absorbed by the gastrointestinal tract. Furthermore, red dots in the figure are for oxadiazole derivatives predicted not to be effluated from the central nervous system by the P-glycoprotein.

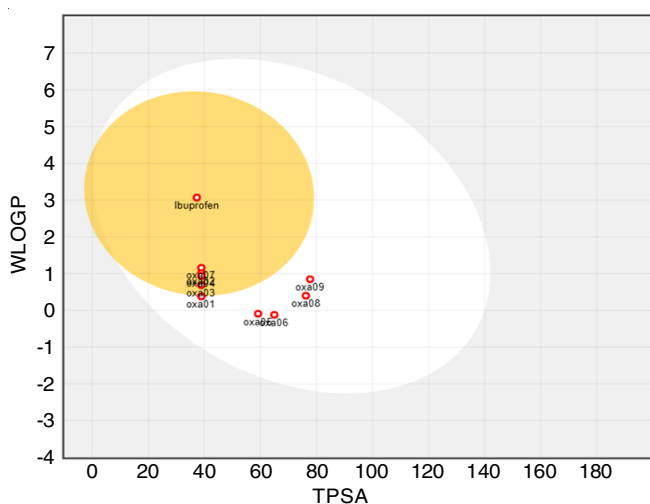


Fig. 7. Boiled egg representation for oxadiazole derivatives including ibuprofen (reference) [Ref. 26]

Conclusion

Solvation dynamics of oxadiazole derivatives in water solvent was performed using *ab initio* Molecular dynamics (MD) and quantum chemistry calculation tools to understand its candidature for the drug preparation based on oxadiazoles as potential candidate. The molecular dynamics study depicts

the total energy as the addition of kinetic as well as potential energies with the progress of simulation time in fs. Both the efficiency of solvation and the main solvent interaction locations for the oxadiazole derivative were studied. The pharmacological properties of different derivatives were also studied.

ACKNOWLEDGEMENTS

One of the authors, SK, thanks Magadh University, Bodh Gaya, India for providing the laboratory facilities and Science and Engineering Research Board (SERB), Department of Science and Technology (DST), India (Grant No. SRG/2019/002284) for financial support.

CONFLICT OF INTEREST

The authors declare that there is no conflict of interests regarding the publication of this article.

REFERENCES

- J. Boström, A. Hogner, A. Llinàs, E. Wellner and A.T. Plowright, *J. Med. Chem.*, **55**, 1817 (2012); <https://doi.org/10.1021/jm2013248>
- C.S. De Oliveira, B.F. Lira, J.M. Barbosa-Filho, J.G.F. Lorenzo and P.F. De Athayde-Filho, *Molecules*, **17**, 10192 (2012); <https://doi.org/10.3390/molecules170910192>
- A. Siwach and P.K. Verma, *BMC Chem.*, **14**, 70 (2020); <https://doi.org/10.1186/s13065-020-00721-2>
- E.M. Lenz, A. Kenyon, S. Martin, D. Temesi, J. Clarkson-Jones and H. Tomkinson, *J. Pharm. Biomed. Anal.*, **55**, 500 (2011); <https://doi.org/10.1016/j.jpba.2011.02.005>
- S. Bala, S. Kamboj, A. Kajal, V. Saini and D.N. Prasad, *BioMed Res. Int.*, **2014**, 172791 (2014); <https://doi.org/10.1155/2014/172791>
- L. Wang, J. Cao, Q. Chen and M. He, *J. Org. Chem.*, **80**, 4743 (2015); <https://doi.org/10.1021/acs.joc.5b00207>
- M.Y. Wong, S. Krotkus, G. Copley, W. Li, C. Murawski, D. Hall, G.J. Hedley, M. Jaricot, D.B. Cordes, A.M.Z. Slawin, Y. Olivier, D. Beljonne, L. Muccioli, M. Moral, J.-C. Sancho-Garcia, M.C. Gather, I.D.W. Samuel and E. Zysman-Colman, *ACS Appl. Mater. Interfaces*, **10**, 33360 (2018); <https://doi.org/10.1021/acsami.8b11136>
- M.J. Buzón, M. Massanella, J.M. Llibre, A. Esteve, V. Dahl, M.C. Puertas, J.M. Gatell, P. Domingo, R. Paredes, M. Sharkey, M. Stevenson, S. Palmer, B. Clotet, J. Blanco and J. Martinez-Picado, *Nat. Med.*, **16**, 460 (2010); <https://doi.org/10.1038/nm.2111>
- N.D. James, H. Payne, M. Borre, B.A. Zonnenberg, P. Beuzebec, A. Caty, S. McIntosh, T. Morris, D. Phung and N.A. Dawson, *BJU Int.*, **106**, 966 (2010); <https://doi.org/10.1111/j.1464-410X.2010.09638.x>
- S. Vardan, H. Smulyan, S. Mookherjee and R. Eich, *Clin. Pharmacol. Ther.*, **34**, 290 (1983); <https://doi.org/10.1038/clpt.1983.170>
- J. Janardhanan, M. Chang and S. Mobashery, *Curr. Opin. Microbiol.*, **33**, 13 (2016); <https://doi.org/10.1016/j.mib.2016.05.009>
- M.A. Ali and M. Shaharyar, *Bioorg. Med. Chem. Lett.*, **17**, 3314 (2007); <https://doi.org/10.1016/j.bmcl.2007.04.004>
- Z. Peng, Z. Bao and M.E. Galvin, *Adv. Mater.*, **10**, 680 (1998); [https://doi.org/10.1002/\(SICI\)1521-4095\(199806\)10:9<680::AID-ADMA680>3.0.CO;2-H](https://doi.org/10.1002/(SICI)1521-4095(199806)10:9<680::AID-ADMA680>3.0.CO;2-H)
- X.-C. Li, A.B. Holmes, A. Kraft, S.C. Moratti, G.C.W. Spencer, F. Cacialli, J. Grüner and R.H. Friend, *J. Chem. Soc. Chem. Commun.*, 2211 (1995); <https://doi.org/10.1039/C39950002211>
- H.N. Bhagavan and R.K. Chopra, *Mitochondrion*, **7**, S78 (2007); <https://doi.org/10.1016/j.mito.2007.03.003>

16. G.K.H. Tam, S.M. Charbonneau, F. Bryce, C. Pomroy and E. Sandi, *Toxicol. Appl. Pharmacol.*, **50**, 319 (1979); [https://doi.org/10.1016/0041-008X\(79\)90157-1](https://doi.org/10.1016/0041-008X(79)90157-1)
17. F. Neese, *Wiley Interdiscip. Rev. Comput. Mol. Sci.*, **2**, 73 (2012); <https://doi.org/10.1002/wcms.81>
18. F. Neese, *Wiley Interdiscip. Rev. Comput. Mol. Sci.*, **12**, e1606 (2022); <https://doi.org/10.1002/wcms.1606>
19. P. Fuentealba, P. Pérez and R. Contreras, *J. Chem. Phys.*, **113**, 2544 (2000); <https://doi.org/10.1063/1.1305879>
20. P.W. Ayers and R.G. Parr, *J. Am. Chem. Soc.*, **122**, 2010 (2000); <https://doi.org/10.1021/ja9924039>
21. W. Yang and R.G. Parr, *Proc. Natl. Acad. Sci. USA*, **82**, 6723 (1985); <https://doi.org/10.1073/pnas.82.20.6723>
22. R. Ahlrichs, M. Bär, M. Häser, H. Horn and C. Kölmel, *Chem. Phys. Lett.*, **162**, 165 (1989); [https://doi.org/10.1016/0009-2614\(89\)85118-8](https://doi.org/10.1016/0009-2614(89)85118-8)
23. C. Steffen, K. Thomas, U. Huniar, A. Hellweg, O. Rubner and A. Schroer, *J. Comput. Chem.*, **31**, 2967 (2010); <https://doi.org/10.1002/jcc.21576>
24. A. Daina, O. Michielin and V. Zoete, *Sci. Rep.*, **7**, 42717 (2017); <https://doi.org/10.1038/srep42717>
25. A. Daina, O. Michielin and V. Zoete, *J. Chem. Inf. Model.*, **54**, 3284 (2014); <https://doi.org/10.1021/ci500467k>
26. A. Daina and V. Zoete, *ChemMedChem*, **11**, 1117 (2016); <https://doi.org/10.1002/cmdc.201600182>
27. A. Zarrouk, B. Hammouti, A. Dafali, M. Bouachrine, H. Zarrok, S. Boukhris and S.S. Al-Deyab, *J. Saudi Chem. Soc.*, **18**, 450 (2014); <https://doi.org/10.1016/j.jscs.2011.09.011>
28. H. Wang, X. Wang, H. Wang, L. Wang and A. Liu, *J. Mol. Model.*, **13**, 147 (2006); <https://doi.org/10.1007/s00894-006-0135-x>
29. A. Mishra, C. Verma, H. Lgaz, V. Srivastava, M. Quraishi and E.E. Ebenso, *J. Mol. Liq.*, **251**, 317 (2018); <https://doi.org/10.1016/j.molliq.2017.12.011>
30. E.E. Ebenso, T. Arslan, F. Kandemirli, I. Love, C. Ögretir, M. Saracoglu and S.A. Umoren, *Int. J. Quantum Chem.*, **110**, 2614 (2010); <https://doi.org/10.1002/qua.22430>
31. M. El Azzouzi, A. Aouniti, S. Tighadouin, H. Elmsellem, S. Radi, B. Hammouti, A. El Assyry, F. Bentiss and A. Zarrouk, *J. Mol. Liq.*, **221**, 633 (2016); <https://doi.org/10.1016/j.molliq.2016.06.007>